

Modeling of Radar Absorbing Materials Using Winning Particle Optimization Applied on Electrically Conductive Nanostructured Composite Material

Davide Micheli, Roberto Pastore, Mario Marchetti

Department of Astronautic, Electric and Energy, Sapienza University of Rome
Roma, Italy

davide.micheli@uniroma1.it; roberto.past@gmail.com; mario.marchetti@uniroma1.it

Abstract- Modelling and manufacturing of radar absorbing material are proposed using multilayer composite nanostructured materials and the recently introduced winning particle optimization algorithm. The study concerns tile of materials with dimensions of 0.3m×0.3m made of nanostructured composite materials, which consist on epoxy-resin and industrial grade carbon nanotube (CNTs) fillers. The industrial grade CNTs were appositely chosen for their low costs, in order to be applied in great amount to build large tile of composite materials. Here modelling takes into account for an extended frequency band (5 to 18 GHz), for several incidence angles of the electromagnetic field (0 to 80°), and for the minimization of the electromagnetic reflection coefficient. At last simulations are compared with measurements of reflection coefficient. Despite some errors mostly due to the manufacturing process, simulations are in good agreement with measurements, showing an interesting approach to design multilayer radar absorbing materials.

Keywords- Radar Absorbing Materials; Evolutionary Computation; Winning Particle Optimization; Modding; Carbon Nanotubes; Composite Nanostructured Materials; Layered Structures; Non-Destructive Testing; NRL-Arch; Stealth

I. INTRODUCTION

Radar absorbing materials (RAM) acquired importance since their first applications in military field [1-6]. Germany pioneered the first aircraft to use RAM during World War II, in the form of the “Horten Ho 229”, in order to reduce the radar signature, and concerned with radar camouflage for submarines, developed “Wesch” material, a carbonyl iron powder loaded rubber sheet about 0.3 inches thick and a resonant frequency at 3 GHz. Composite materials considered in this work are based on epoxy matrix reinforced with carbon nanomaterials. These latter were chosen taking into account their good microwave absorption behaviour [7] and the low market prices. In fact, the economic aspects, normally neglected in small laboratory applications, are important in real applications where the amount of carbon nanopowders fillers could be relatively high. In such scenario, a good compromise in terms of cost/performances was obtained using industrial grade multiwall carbon nanotubes (MWCNTs) with a cost of about 300 \$/kg. MWCNTs with commercial name of NANOCYLTM NC7000 (diameter around 9.5 nm, length 1.5 μm, purity 90%) were bought at NANOCYL. Bi-component Epoxy-resin PrimeTM 20LV (density 1.123 g/cm³) with Hardner (density 0.936 g/cm³) was used as matrix. RAM is based on layered materials where each layer is made of carbon nanostructured composites materials in different weight percentages. The recent developed winning particle optimization search

algorithm (WPO) was applied in order to design and optimize multilayer materials able to effectively absorb microwaves in the range 5 GHz to 18 GHz. The paper is organized in 5 distinct sections. In Section II, mathematical model of absorber is shown; in Section III, WPO is described; in Section IV, numerical design of RAM is discussed and in Section V, RAM manufacturing and electro magnetic performance comparisons between simulation and manufactured RAM are shown. In this section the adopted experimental setup is accurately described showing the NRL-arch test fixture. It is crucial to highlight the interdisciplinary research activity through nanomaterials, electro magnetic wave propagation theory, composite materials manufacturing techniques and search computation algorithms. All of them are required to design the “quasi perfect absorber”.

II. RAM MATHEMATICAL MODEL

WPO algorithm [8-9], has been applied to solve a quite complex problem consisting in the design and optimization of microwave absorbing multilayer materials.

Optimized RAM is based on nanomaterials in particular carbon nanostructured composites materials. Conductive fillers have been uniformly dispersed in an epoxy resin at different weight percentages (0.5, 1, 2, 2.5, 3 wt %). In Table I, six different composite materials and the index code adopted by WPO to identify each material are shown.

TABLE I
CODING OF MATERIALS IN THE DATA BASE

Materials	Materials Code
Epoxy- Resin	1
MWCNT, 0.5 wt%	2
MWCNT, 1.0 wt%	3
MWCNT, 2.0 wt%	4
MWCNT, 2.5 wt%	5
MWCNT, 3.0 wt%	6

The resulting composites samples have been dielectrically characterized in a previous work [10-11] by waveguide measurements to recover the dielectric properties of the composite materials in the data base (DB). In this paper the DB of these dielectric parameters as function of frequency is used to supply the WPO modeling algorithm. In Table II, a brief summary of the dielectric permittivity of composite materials at 6GHz, 12 GHz, 18 GHz, is shown. After that, numerical simulations of RAM have been carried out. In particular, electromagnetic analysis has been performed integrating the

forward/backward propagation formalism to the *in-house* built WPO, thus able to carry out optimization upon oblique incidence angles over a finite angular range.

TABLE II DIELECTRIC PERMITTIVITY OF COMPOSITE NANOSTRUCTURED MATERIALS

Materials	Real Part and Imaginary Part					
	F1= 6 Ghz	F2= 12 Ghz	F3=18 Ghz			
Epoxy- Resin	3.11	0.10	3.07	0.08	3.07	0.08
MWCNT, 0.5 Wt%	5.52;	0.90	5.33	1.81	5.21	2.83
MWCNT, 1.0 Wt%	9.52	5.27	6.75	2.88	5.39	1.95
MWCNT, 2.0 Wt%	11.42	6.89	8.82	4.48	7.45	3.38
MWCNT, 2.5 Wt%	12.90	11.28	10.86	10.35	9.71	9.79
MWCNT, 3.0 Wt%	18.21	14.50	17.29	13.65	16.72	13.31

The developed code minimizes reflection and transmission coefficients under the thickness minimization constraint. Finally, *broadband quasi-perfect absorbers* in the band 5-18 GHz are achieved combining the filler families, i.e., exhibiting a loss factor (*LF%*) greater than 90% in most of the band, for thicknesses ranging between 5 and 12 mm. Main goal of design and optimization work was to achieve values (< -10 dB) of reflection coefficients (*RC*), for angular apertures within 40° in the most part of the frequency band. The design/optimization is basically a *minimization* procedure which seeks the best trade-off between structure thickness (to be minimized) and absorbed EM power (to be maximized). The absorbing power has been quantified through the so-called "loss factor" *LF%*, defined as follows [10-11].

$$LF\% = (1 - |RC|^2 - |TC|^2) \cdot 100. \quad (1)$$

In RAM systems the transmission coefficient *TC*=0 (because of the perfect electric conductor (PEC) layer at the end of the multilayer), and the *RC* is the WPO-optimized reflection coefficient.

Both are expressed in the linear form. *LF%* physical meaning is related to the fraction of the incident power vanishing inside the materials because of localization and dissipation phenomena. Since the calculation of *RC* becomes a crucial point for RAM optimization goal, a rigorous approach for computing reflected waves at each layer has been adopted [11-13].

Both normal and oblique incidences have been evaluated during the automatic optimization. In Fig. 1, a general scheme of the electromagnetic absorbing multilayer structure is presented. Each layer is generally denoted by index *x*.

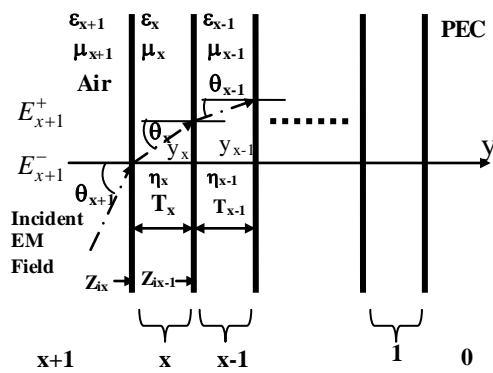


Fig. 1 General Multilayer scheme of electromagnetic absorbing structure; in RAM systemsthe back layer is a perfect electric conductor (PEC).

As far as geometric properties of multilayer structures are concerned, thickness of each layer can range from 0 to 10 mm, while the number of layers is upper-bounded to *maximum* 10 layers. The effective number of layers is established by the WPO optimization procedure which is able to remove one or more useless layers from the multilayer structure. The order of layer materials is not *a priori* fixed; instead WPO algorithm decides which material need to be used for each layer.

In RAM applications, *RC* at the air-absorber interface can be evaluated by the following equation relating the free space impedance to the input impedance seen at the air-multilayer structure interface

$$RC^{TM/TE} = \frac{Z_i^{TM/TE} - Z_0^{TM/TE}}{Z_i^{TM/TE} + Z_0^{TM/TE}}, \quad (3)$$

$$RC_{dB}^{TM/TE} = 20 \log_{10} \left| \frac{Z_i^{TM/TE} - Z_0^{TM/TE}}{Z_i^{TM/TE} + Z_0^{TM/TE}} \right|$$

where $Z_0 \approx 377 \Omega$ is the free space impedance and Z_i is the input impedance at the first air-absorber interface. The input wave impedance of the multilayer, backed by PEC, can be expressed iterating the following equation for *x*-th-layer [11-13].

$$Z_{ix}^{TM/TE} = \eta_x^{TM/TE} \frac{Z_{ix-1}^{TM/TE} \cos(k_x t_x) + j \eta_x^{TM/TE} \sin(k_x t_x)}{\eta_x^{TM/TE} \cos(k_x t_x) + j Z_{ix-1}^{TM/TE} \sin(k_x t_x)} \quad (4)$$

In (4), $t_x = y_{x-1} - y_x$ is the *x*-th layer thickness expressed in m, whereas the wave number k_x of each layer along *y* axes is

$$k_x^2 = (2\pi f)^2 \mu_0 \epsilon_0 \mu_{rx} \epsilon_{rx} \cos^2 \vartheta_x = \\ (2\pi f)^2 \mu_0 \epsilon_0 \mu_{rx} (\epsilon_{rx}' - j \epsilon_{rx}'') \cos^2 \vartheta_x \quad (5)$$

where *f* is frequency of the incident electromagnetic wave in Hz, ϵ' is the real part of *x*-th-layer permittivity and ϵ'' is the imaginary part of layer permittivity.

Complex waves appear in oblique incidence and lossy dielectrics problems [13]. Because of the wave number become complex-valued, e.g., $\bar{k} = \bar{\beta} - j\bar{\alpha}$, the angle of refraction and possibly the angle of incidence may become complex-valued too. In calculating k_x by taking square root of (5), it is required, in complex-wave problems, to get the correct signs of their imaginary parts, such that evanescent waves are described correctly. This leads to define an "evanescent" square root as follows. Let $\epsilon_{rx} = (\epsilon_{rx}' - j \epsilon_{rx}'')$ with $\epsilon_{rx}'' > 0$ for an absorbing medium, then

$$k_x^2 = \begin{cases} \sqrt{(2\pi f)^2 \mu_0 \epsilon_0 \mu_{rx} (\epsilon_{rx}' - j \epsilon_{rx}'') \cos^2 \vartheta_x}, & \text{if } \epsilon_{rx}'' > 0 \\ -j\sqrt{-(2\pi f)^2 \mu_0 \epsilon_0 \mu_{rx} (\epsilon_{rx}') \cos^2 \vartheta_x}, & \text{if } \epsilon_{rx}'' = 0 \end{cases} \quad (6)$$

Since all nanostructured composite materials available in the DB are with $\epsilon_{rx}'' > 0$ then k_x is as usually computed.

III. WINNING PARTICLE OPTIMIZATION

WPO is a simple algorithm where at each time epoch of evolution, the particle, which best fit the objective function, is deputed to pilot the trajectory of the remaining particles within the multidimensional space of solutions, i.e., variables to be optimized. In Fig. 2, WPO flow chart is shown. At the

beginning of the iterations, particles are randomly distributed within the n -dimensional search space.

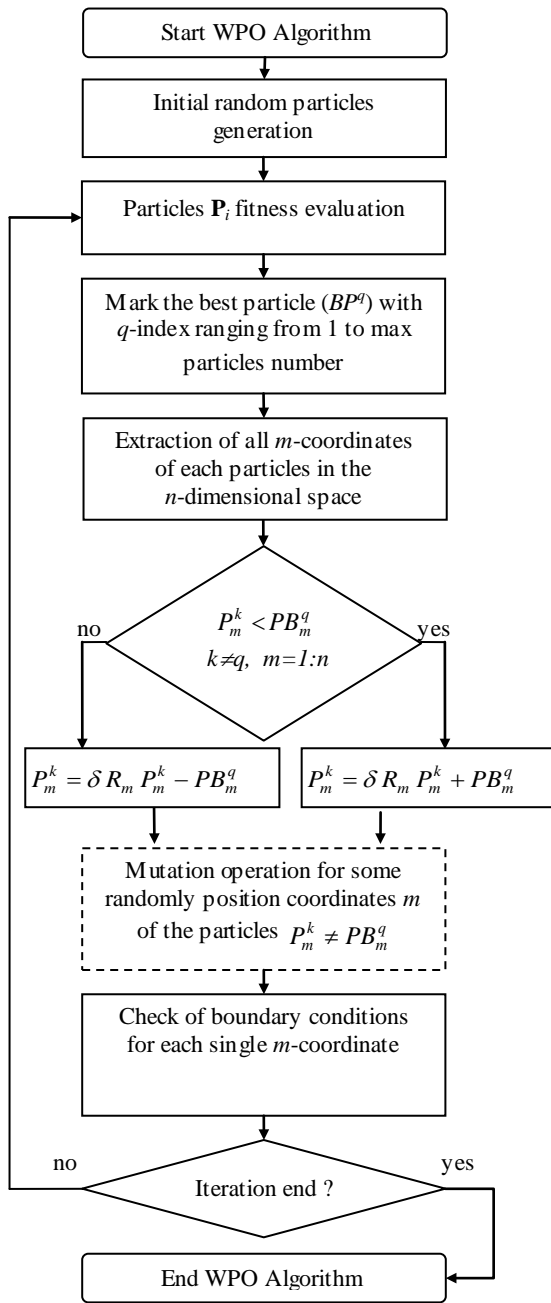


Fig. 2 WPO flow chart

At each iteration time, the objective function of each particle is computed. Then, particles are compared to each other using value of their objective function and the best fitting particle is marked with its proper index. Each particle position is completely defined by its coordinates and their number represents the dimension of the space where all particles jump searching for the optimal solution. Trajectory of each particle, except that of the best fitting particle, is defined in the following way: if m th-coordinate of a certain particle P^k is lesser than the corresponding m th-coordinate of the current best particle PB^q , then the new m th-coordinate will result from the sum of current particle and best particle m th-coordinates; while if m th-coordinate of a certain particle P^k is greater than the corresponding m th-coordinate of the current best particle PB^q , then the new m th-coordinate will result from the difference

between the current particle m th-coordinates and the best particle m th-coordinates. Here, q is the index of the best particle found in each iteration and the condition which needs to be grant is $q \neq k$, i.e., all k th particles can be displaced except the best q th particle. Equation (7) describes the mentioned approach. Particle position at the $(i+1)$ th iteration as a function of particle position in the previous i th iteration is.

$$P_m^k(i+1) = \delta R_m P_m^k(i) + g PB_m^q(i) \quad (7)$$

where

$$g = +1 \text{ if } P_m^k(i) < PB_m^q(i)$$

$$g = -1 \text{ if } P_m^k(i) > PB_m^q(i)$$

k = Particle index in the range [1, Particle Number]

q = Best Particle index in the range [1, Particle Number]

and $k \neq q$

m = ranges in [1, n]

n = Space Dimensions

R_m = random number in the interval [0, 1]

δ = Convergence Parameter

i = current iteration in the range [1, N]

N = Number of iteration

R_m is used to randomly define the amount of displacement of each single coordinate. Such randomization develops the searching ability by conferring some causality to the amplitude of jumps. Convergence parameter δ helps the final convergence of the WPO algorithm as follows. At the beginning of the iterations, the WPO must be capable to explore the largest space of solutions as possible. On the other hand, close to the end of the iterations, high amplitude of jumps could represent a drawback since a position representing the optimal solution could forbid. In order to improve the WPO convergence, a mechanism providing a progressive reduction of "maximum jumps amplitude" has been introduced and it is identified by the δ parameter. Calling N the total number of iterations and supposing i the current iteration, then the value of δ is given by

$$\delta = \sigma \left(1 - \frac{i}{N+1} \right)^S \quad (8)$$

$$\sigma = J(R_m - 0.5) \quad (9)$$

where J is the "jump amplitude" defined by the user as a numerical parameter in the main program of WPO, in this scenario it has been valued to 3 after several trials to assure a good performance in domain solution exploration.

In (8), the meaning of σ and S parameters is in fast or slow convergence of the WPO algorithm. In particular, the higher the σ , the greater the initial jumps amplitude and the greater the distances where particles will start to explore the search space. As far as S is concerned the higher its value, the faster the convergence to a suboptimal solution. The parameter σ is made using J and R_m such that $(R_m - 0.5)$ is a random number between $[-1/2, +1/2]$. The random part of σ develops the search capability of the algorithm. Even though mutation operation has not been applied on the subsequent reported optimizations (mutation=0%), it has to be noticed that mutation can be included in WPO algorithm to further increase the random search capability. At the end of each WPO iteration, checking of boundary conditions for the new set of particles coordinates

is computed in order to avoid overcoming the constraints. The entire loop cycle can be iterated several times in order to get the required objective function minimization.

IV. RAM DESIGN AND OPTIMIZATION

The presented modeling procedure, takes into account for several incidence angles and, the design/optimization procedure can be forced to run for a one particular incidence angle or for a range of angular incidences where the global objective function has to be optimized. In particular the incidence angles here range between 0° and 80° with step 10°. As far as layer materials are concerned each one can be chosen among all of different manufactured composite materials. In Table I, all the composite materials available in the DB are reported and each composite material has been coded using an integer number.

WPO can access to DB in order to allocate the most appropriate materials for each layer of the multilayer RAM. In WPO procedures the modeling functions are called by the main program to compute: materials intrinsic impedances, in-outgoing refraction angle, TE/TM layer wave impedance, reflection coefficient (RC), and the loss factor (LF). The multilayer absorbing structures considered in the design procedure can have up to 10 layers so dimensionality of layer space is 10 i.e., $m = 10, 9 \dots 1$.

Since the optimization are for both: layer thickness and layer material type then WPO algorithms need to be structured in order to take into account for both quantities.

In WPO algorithm we have: $T^k(i) = [t_{10}^k(i), t_9^k(i), \dots, t_1^k(i)]$, as array of thicknesses, where $T_m^k(i)$ is the thickness of m -th layer, and $P^k(i) = [p_{10}^k(i), p_9^k(i), \dots, p_1^k(i)]$, as array of material type, where $P_m^k(i)$ is the type of material associated to the m th layer.

The equations related to layer thicknesses and layer material for each single particle are simply updated according to,

$$\begin{aligned} T_m^k(i+1) &= \delta R_{m1} T_m^k(i) + g_{Thickness} TB_m^q(i) \\ P_m^k(i+1) &= \text{round}(\delta R_{m2} P_m^k(i) + g_{Material} PB_m^q(i)) \end{aligned} \quad (10)$$

Where, R_{m1} and R_{m2} are random numbers in the closed range 0-1, $T_m^k(i)$ is the current k th-particle, m th-layer-thickness at the i th-iteration, while $P_m^k(i)$ is the current k th-particle, m th-layer-material at the i th-iteration.

Rounded values in material equation are required since the index of material of each layer must be an integer number ranging from 1 to the number of materials available in the DB of materials.

$$\begin{aligned} g_{Thickness} &= +1 \text{ if } T_m^k(i) < TB_m^q(i) \\ &= -1 \text{ if } T_m^k(i) > TB_m^q(i) \\ g_{Material} &= +1 \text{ if } P_m^k(i) < PB_m^q(i) \\ &= -1 \text{ if } P_m^k(i) > PB_m^q(i) \end{aligned} \quad (11)$$

where q is the index of best particles TB and PB ; k is the index of particles with $k \neq q$; n is the dimension number; m is the current dimension ranging between $[1, n]$. In the presented

implementation, the value of convergence parameter S is set to 1.

WPO try to minimize a global objective function (GOF) which in turn is built using elementary objective functions (EOF). The EOF for TM and TE modes are named as $CostRC_{TM}$, $CostRC_{TE}$, for reflection coefficient. The formal definition of the EOF for TM and TE modes are shown in (12),(13),(14). We can observe that for each particle (Pa), the corresponding EOF is evaluated over the entire frequency band and over the entire incidence angular range, adopting frequency and angular steps chosen by the user before starting the WPO,

$$\begin{aligned} CostRC_{TM}(Pa) &= \left[\sum_{freq=f \min}^{freq=f \ max} \left(\sum_{\theta=\theta \ min}^{\theta=\theta \ max} RC_{TM}(Pa, freq, \theta) \right) \right] \\ CostRC_{TE}(Pa) &= \left[\sum_{freq=f \ min}^{freq=f \ max} \left(\sum_{\theta=\theta \ min}^{\theta=\theta \ max} RC_{TE}(Pa, freq, \theta) \right) \right] \end{aligned} \quad (12)$$

where Pa is the current particle, $freq$ is the frequency step, $fmin$ and $fmax$ is the frequency band start and stop, θ is the current angular step, θ_{min} and θ_{max} represent the angular range bounds. The definition of the EOF for thickness is

$$CostT(Pa) = [t_{10}(Pa) + t_9(Pa) + \dots + t_1(Pa)] \quad (13)$$

where t_m is the thickness of the m -th layer.

A weighting factor called α ranging in $(0 < \alpha < 1)$, weight CostT w.r.t. CostRC. Such weighting factor is chosen by the user and its meaning have to be intended as the capability of the tool to design the multilayer structure making privilege to the electromagnetic performances w.r.t. the thickness when q is close to 1. Final GOF is a linear combination of the described EOFs,

$$GOF(Pa) = \alpha OF1(Pa) + (1 - \alpha) OF2(Pa) \quad (14)$$

where

$$\begin{aligned} OF1(Pa) &= \left(\frac{CostRC_{TM}(Pa)}{A} + \frac{CostRC_{TE}(Pa)}{A} \right) \\ OF2(Pa) &= \left[\frac{CostT(Pa)}{B} \right] \end{aligned}$$

A and B are normalization factors: A is the product between the frequency step number and the angle step number, whereas B is the product between the maximum layer number and the maximum layer thickness. In the following subsection two RAM models are shown.

A. RAM First Simulation

In the first RAM simulation a weighting factor $\alpha=0.9$ returned the scheme of layered material shown in Fig. 3.

The electromagnetic wave impinges upon the first layer made of epoxy-resin. Incidence and reflection angle is called θ^0 , ranging from 0° to 80°. Total thickness of multilayer RAM is 11.77 mm and the final number of layers is 4. Tile is composed on the top by the lowest lossy material (epoxy-resin) as the first layer up to the highest lossy material in the DB (MWCNTs 3 wt%) as third layer backed by PEC. This structure can be viewed as a graded lossy system in the first three layers and a resonant structure in the fourth layer, where the chosen materials are not the highest lossy materials (MWCNTs 0.5% wt). In particular graded lossy systems are composed by a quasi-wave impedance matched material where the first interface between free space and epoxy-resin is the best coupling material able to assure the lowest reflection

coefficient at the first air-absorber interface. MWCNTs 1wt% and MWCNTs 3wt% instead have lower characteristic wave impedances and greater losses with respect to epoxy-resin and as a consequence they are placed in sequence in the layers order.

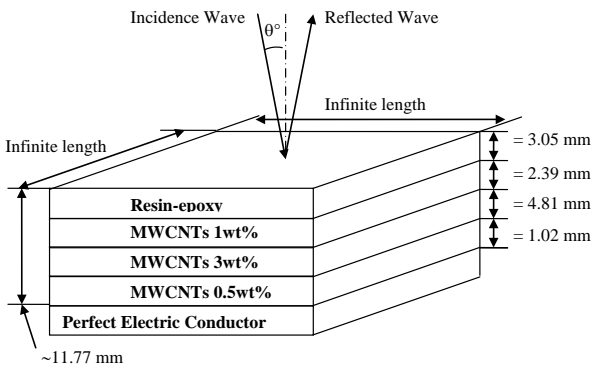


Fig. 3 RAM multilayer simulated: Resin-epoxy, MWCNTs 1wt%, MWCNTs 3wt%, MWCNTs 0.5 wt%, PEC

In Fig. 4, reflection coefficients TE/TM (dB) are shown. It can be noticed that for normal incidence angles, TE and TM curves coincide whereas around 7, 9, 12, 15 GHz, there are some incidence angles where curves show values of reflection coefficient TM even lower with respect to that at normal incidence. Such angles are denoted as Zenneck angles for lossy materials.

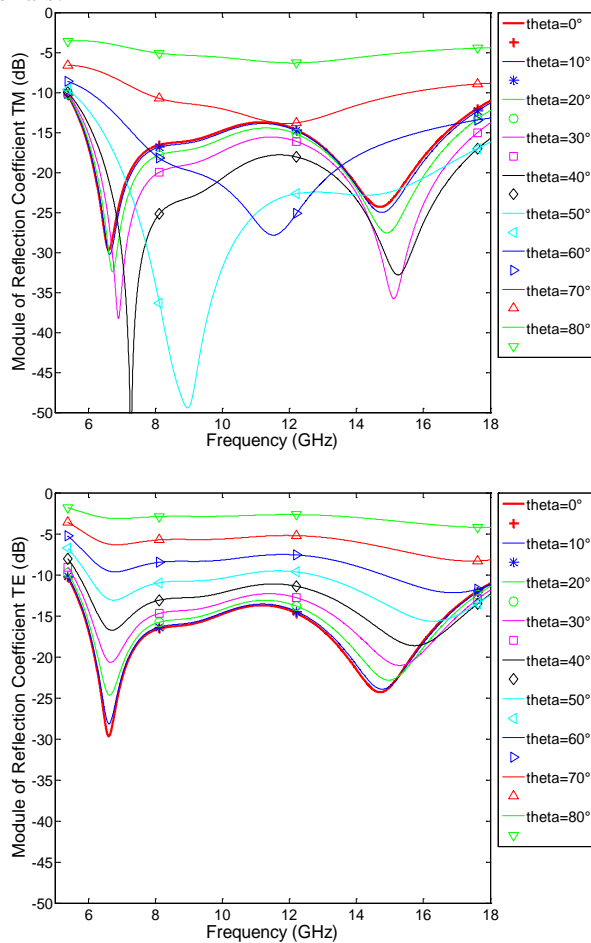


Fig. 4 RAM Reflection Coefficient (dB) TE and TM

The electromagnetic absorbing capability of a certain material is mainly due to two simultaneous conditions: "dielectric losses" within the composite material and

"impedance matching condition" which in turns is a function of thickness of the absorbing layer. The impedance matching condition takes place when the electromagnetic wave impedance at the first interface between air and RAM is close to that of free space i.e., about 377Ω . This is why in the simulation the first layer is logically made of epoxy-resin which possesses the lowest electric permittivity and so the higher electromagnetic wave impedance. The electromagnetic wave impedance at the first interface is computed using (4) and depends on dielectric parameter of all materials in the multilayer. The dielectric losses are described by the imaginary part of the permittivity (ϵ'') while, thickness of the material is connected to the microwave wavelength within the material. The higher the dielectric losses, the greater are the electromagnetic power dissipation phenomena in the RAM composite material. Unfortunately, usually, the higher the dielectric permittivity, the lower is the electromagnetic wave impedance, which in turn mismatch the impedance matching condition with free space [11]. This is why, the RAM is composed of different layers able to progressively match the wave impedance while simultaneously assuring the right dissipation and absorbing behaviour. In Fig. 5, Loss Factor TE/TM is shown. Loss Factor (%) remains above 90% for incidence angles up to 40°. Such values mean that RAM is able to absorb the most part of the electromagnetic field reflecting back only a very little amount of the incoming energy. The extended frequency band 6 to 18 GHz where loss factor is greater than 95%, shows the interesting theoretical performance of this RAM.

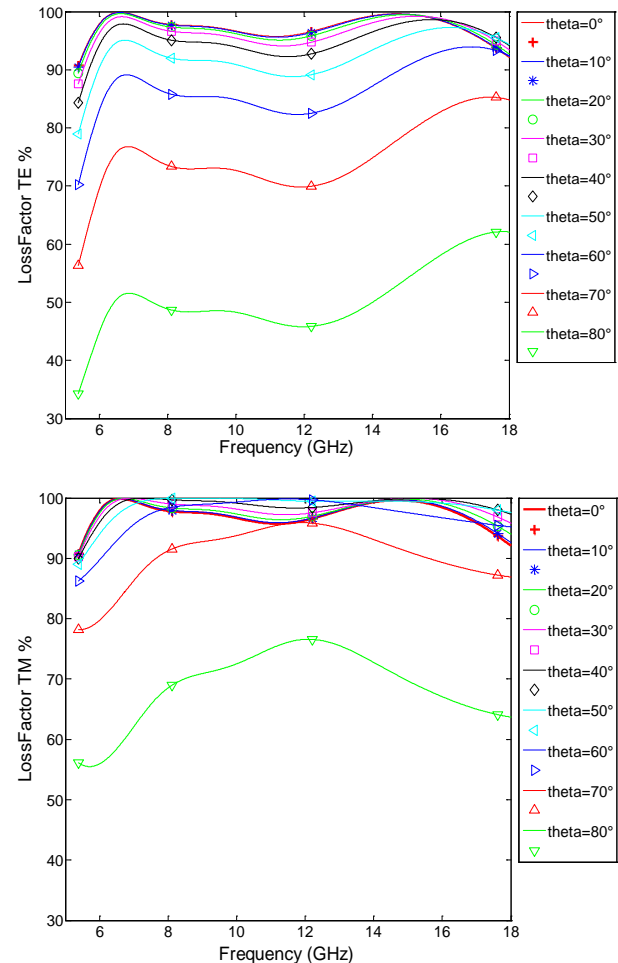


Fig. 5 RAM Loss Factor (%) TE and TM

In Fig. 6, the asymptotic convergence of WPO evolution is shown. Plot of GOF is shown. The simulation is made on 800 iterations and 256 searching particles. The time required to complete the computation strongly depends on the amount of particles and iterations and by the computer performances in terms of random memory allocation and processing speed. After 600 iterations the behaviour of curve is almost asymptotic showing a probably sufficient convergence of the WPO algorithm in searching the best solution to the RAM design and optimization problem. The computing time also depends on the way in which code is written. Here Matlab has been used. Some procedures were parallelized but others require nested loops of cycle to take into account for particles, frequencies, and incidence angles. These are very time consuming.

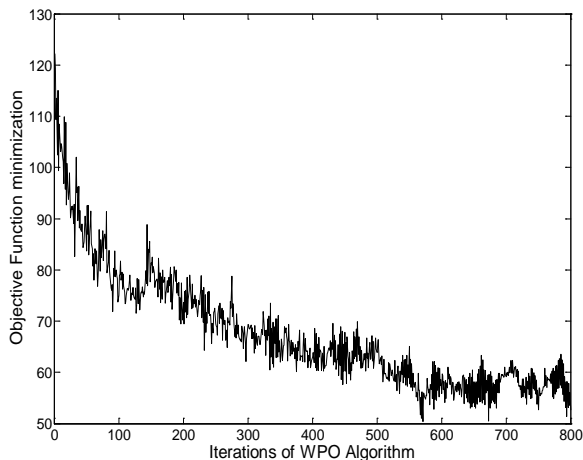


Fig. 6 WPO evolution and convergence

B. RAM Second Simulation

In the second RAM simulation, a lower weighting factor $\alpha=0.6$ returned the scheme of layered materials shown in Fig. 7. The multilayer RAM is composed of three different layers, the first one, where the electromagnetic wave arrives, is epoxy-resin; the second one is made of MWCNTs at 1wt%, the third layer is made of MWCNTs at 2wt%. The total thickness is about 5.72 mm. In Figs. 8 and 9 the electromagnetic performances of RAM are shown.

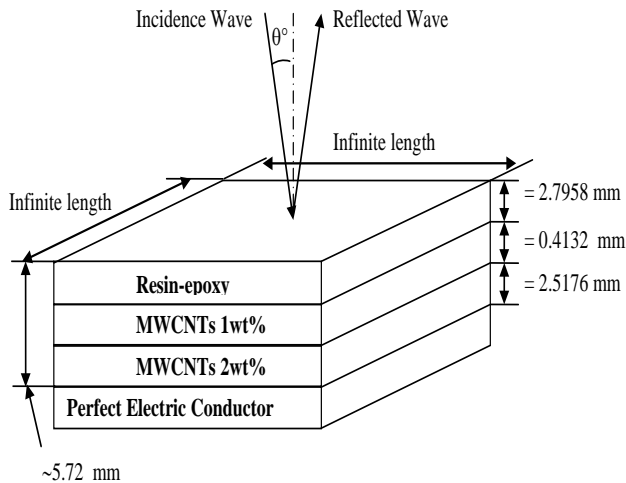


Fig. 7 RAM multilayer simulated: Resin-epoxy MWCNTs 1 wt%, MWCNTs 2wt%, PEC

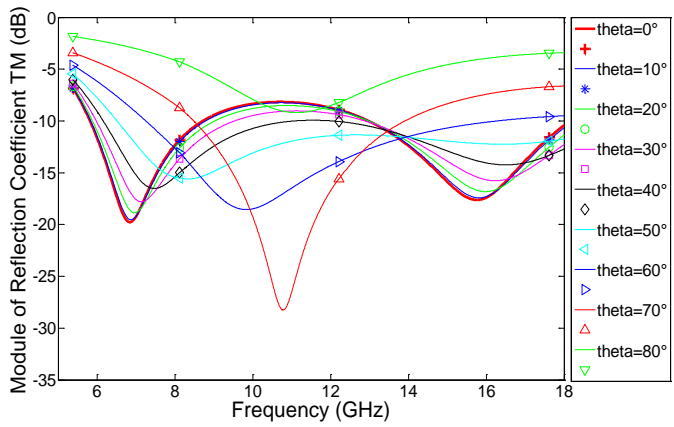
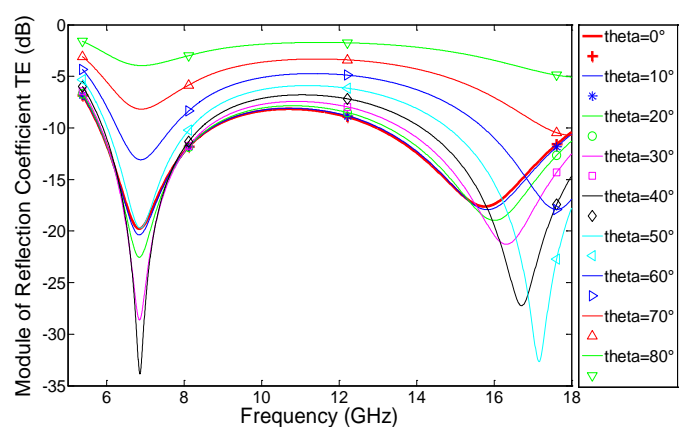


Fig. 8 RAM Reflection Coefficient (dB) TE and TM

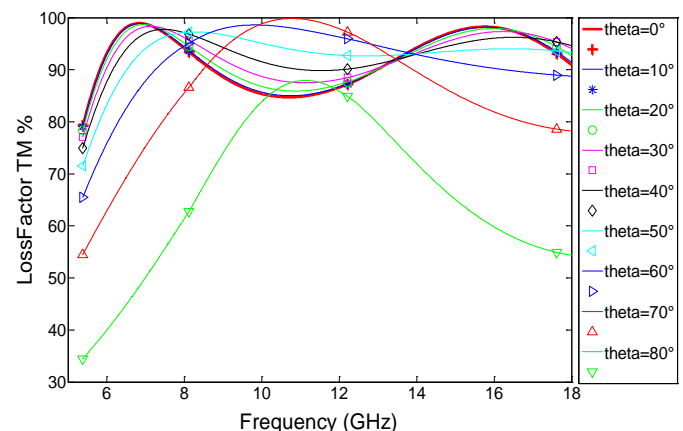
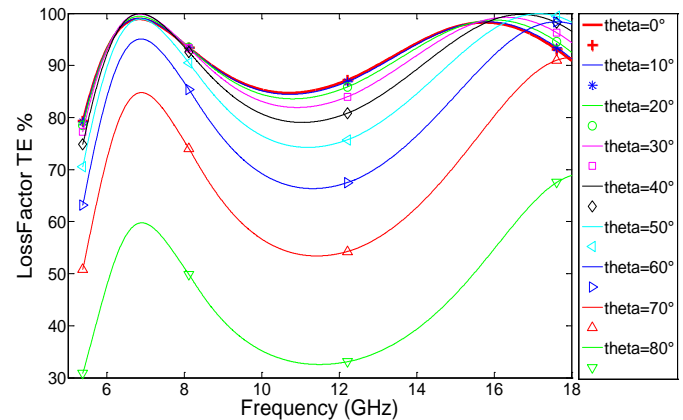


Fig. 9 RAM Loss Factor % TE and TM

The graphs show two peaks of absorption at 0° incidence angle for TE/TM around 7 and 16 GHz. When the incidence angle grows to 50°, 60° and 70° in the TM incidence mode, the first absorption packs shift to 8, 10 and 11 GHz while the second peak disappear.

V . RAM MANUFACTURING AND ELECTROMAGNETIC PERFORMANCE MEASUREMENT

The second simulated RAM multilayer scheme has been chosen as the model to try of building a large RAM tile. Each layer was manufactured over the previous using the sample holder as shown in Fig. 10. The manufacturing procedure is available in [9]. In Fig. 11, the manufactured RAM tile is shown.

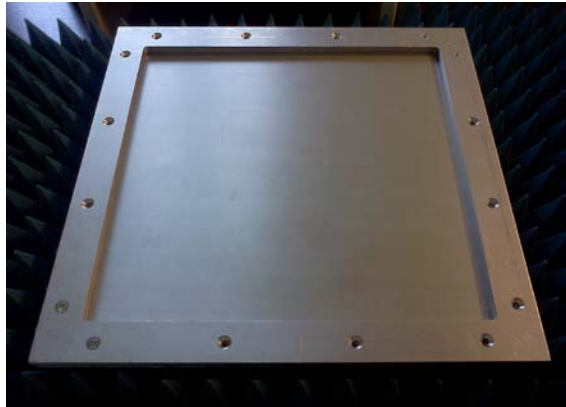


Fig. 10 Sample holder to build multilayer RAM

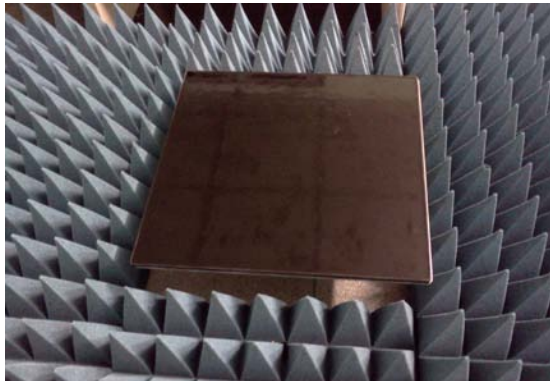


Fig. 11 Final manufactured RAM multilayer tile

The practical realization of the large RAM tile was not easy since the dimensions 30x30 cm required a lot of nanomaterials and the related dispersion process in the epoxy-resin resulted hard. Another very difficult task was to respect the thickness of each layer because the manually homemade deposition of each layer above the other one caused errors in the value of thickness and in the homogeneity of layers along the surface. The great manufacturing problems rose with the layer made of MWCNTs at 2wt%. In fact, such composite doesn't remain enough viscous so tile manufacturing process is quite difficult, especially for respect thickness constraints. At the end, the final manufactured multilayer RAM is lightly different with respect to the initial simulation reported in Fig. 7. In Fig. 12 the manufactured RAM multilayer tile scheme is shown. The total thickness of tile is about 6.1 mm. The simulation of such new tile is shown in Fig. 13. Observing the simulation it can be highlighted that even small variations of thickness layers are able to affect the reflection coefficient lowering the absorption properties of RAM. This is why it is very important to try

respect as much as possible the RAM scheme and thickness performed by WPO simulation, in the case of Fig. 7.

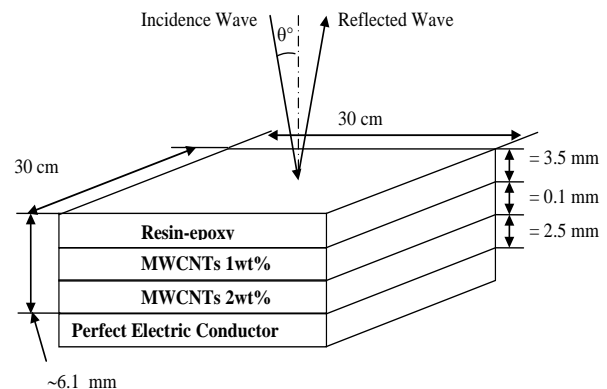


Fig. 12 RAM multilayer manufactured: Resin-epoxy MWCNTs 1 wt%, MWCNTs 2wt%, PEC

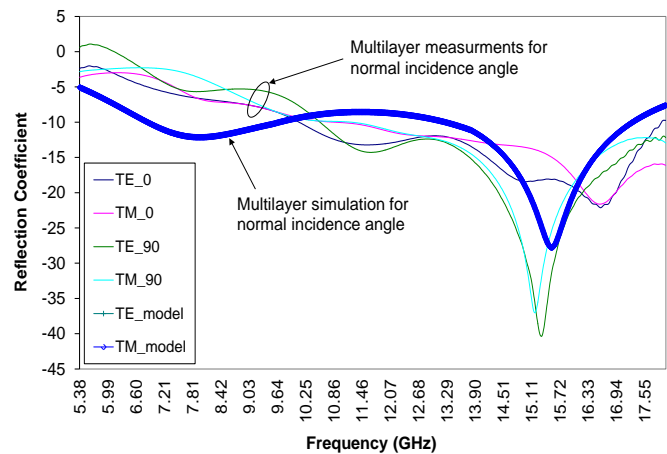


Fig. 13 RAM multilayer manufactured: resin-epoxy MWCNTs 1 wt%, MWCNTs 2wt%, PEC

To evaluate the electromagnetic reflectivity, a NRL arch measurement (bistatic reflection method), has been used [14]. In this configuration, two antennas are placed for transmitting and receiving signals respectively and the microwave reflectivity at different incident angles can be measured. Using this configuration, the reflection properties of materials, can be measured for different incident angles. It should be noted that in bistatic reflection measurements, the reflection is dependent on the polarization of the incident wave. Incident waves with parallel and perpendicular polarization usually result in different reflection coefficients. Besides, special calibration is needed for free-space bistatic reflection measurements [14]. In Fig. 14 bistatic measurement system and the tile in composite material is shown. Bistatic measurement system is here based on Agilent software 8571E (material measurement), and Agilent PNA-L vector network analyser. Antenna used are SATIMO Dual Ridge Horn SH2000 covering the frequency range 2 – 32 GHz. After the calibration of the NRL bistatic system, the reference in reflection coefficient has been taken adopting only metal plate i.e., without RAM tile. After that measurement of a known sample consisting in ECCOSORB AN73 absorber [7], has been performed in order to be aware about errors in the NRL measurement setup. Confidence of measurements was within 2 dB of interval with respect to reflection properties declared in the ECCOSORB data sheet.

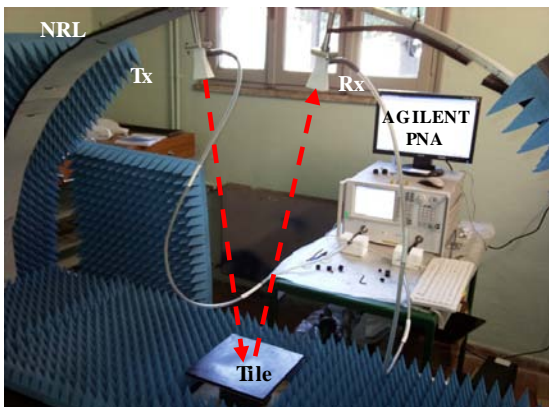


Fig. 14 Bistatic measurement system located at (www.saslab.eu)

Measurement of the manufactured RAM tile using incidence angle of 0° has been performed for TE and TM mode.

In Fig. 14 comparison between simulation of the reflection coefficient of the new manufactured RAM tile and real measurements is shown. The angle of electromagnetic wave incidence is 0°. It can be noticed that the simulated curve shows similar behaviour with respect to the measured one.

Errors and differences in simulated and measured reflection coefficient are mainly due to:

- difficulties in manufacturing RAM multilayer tile where each layer thickness ranges of about 0.5mm between its minimum to its maximum value; so the reported value represent an average value. To be aware of the manufacturing errors, in Fig. 14 we show the measurements of RAM called TE_0, TM_0, TE_90, TM_90. The numbers 0 and 90 mean that the RAM tile placed on the metal plate was rotated respectively of 0° and 90°. It can be noticed that there are some differences in the measured reflection coefficients which can be explained by errors in the manufacturing process.
- accuracy in determination of permittivity of composite materials performed using wave guide method.
- accuracy in free space measurement of reflection coefficient using bistatic method.

V. CONCLUSION

In this work modelling, optimization and manufacturing of radar absorbing materials have been discussed. The design and optimization took place using the recently introduced winning particle optimization search algorithm which has been applied to optimize the electromagnetic absorbing properties while contemporaneously minimizing the overall thickness of multilayer material. Following the simulation, a large tile of radar absorbing material has been manufactured by using industrial grade of multiwall carbon nanotubes and measurement of electromagnetic reflection coefficient performed by NRL-arch. Comparison between simulation and measurement show interesting agreement. Nevertheless some errors occurred in manufacturing process which affected electromagnetic performances of manufactured radar absorbing material.

REFERENCES

- [1] Lederer, P. G. *An Introduction to Radar Absorbent Materials (RAM)*, Royal Signals and Radar Establishment, Malvern, 1986.
- [2] Vinoy, K. J.; Jha, R. M. *Radar Absorbing Materials: From theory to Design and Characterization*, Kluwer Academic Publishers: Boston, 1996.
- [3] Knott, E. F.; Shaeffer, J. F.; Tuley, M. T. *Radar Cross Section*, 2Rev. ed ed.; Artech House: Norwood, 1993.
- [4] Ruck, G. T. *Radar Cross Section Handbook*; Vol.II, Plenum Press: New York, 1970.
- [5] Andrei Shepelev and Huib Ottens, *Horten Ho 229 Spirit of Thuringia: The Horten All-Wing Jet Fighter*, Lan Allan Publishing Ltd, Hersham, Surrey KT12 4RG. 2006.
- [6] Paul Saville, "Review of Radar Absorbing Materials", *Defence R&D Canada – Atlantic*, 2005.
- [7] Davide Micheli, Carmelo Apollo, Roberto Pastore, Ramon Bueno Morlesa, Susanna Laurenzi, Mario Marchetti, "Nanostructured Composite Material for Electromagnetic Interference Shielding Applications", *Acta Astronautica, Science Direct, Elsevier*, 2011.
- [8] Davide Micheli, Carmelo Apollo, Roberto Pastore, Ramon Bueno Morlesa, Daniele Barbera, Mario Marchetti, Gabriele Gradoni, Valter Mariani Primiani, and Franco Moglie, "Optimization of Multilayer Shields Made of Composite Nanostructured Materials", *IEEE TRANSACTIONS ON ELECTROMAGNETIC COMPATIBILITY*, 2011.
- [9] Davide Micheli, *Radar Absorbing Materials and Microwave Shielding Structure Design*, LAP Lambert Academic Publishing, 2012.
- [10] Davide Micheli, Roberto Pastore, Carmelo Apollo, Mario Marchetti, Gabriele Gradoni, Valter Mariani Primiani, and Franco Moglie, "Broadband Electromagnetic Absorbers using Carbon Nanostructure-Based Composites", *IEEE Transactions on Microwave Theory and Techniques*, 2011.
- [11] Davide Micheli, Roberto Pastore, Carmelo Apollo, Mario Marchetti, "X-Band microwave characterization of carbon-based nanocomposite material, absorption capability comparison and RAS design simulation", *Composites Science and Technology*, 2009.
- [12] J. A. Kong, *Electromagnetic Wave Theory*. New York: Wiley, 1986.
- [13] J. A. Stratton, *Electromagnetic Theory*. Hoboken, NJ:Wiley-IEEE Press, 2007.
- [14] M. H. Umari, D. K. Ghodgaonkar, V. V. Varadan, and V. K. Varadan, "A free-space bistatic calibration technique for the measurement of parallel and perpendicular reflection coefficients of planar samples," *IEEE Trans Instrum. Meas.*, vol. 40, no. 1, pp. 19–24, 1991.



Davide Micheli was born in Ancona, Italy, in 1967. He received the University degree in electronics engineering from the University of Ancona (now Università Politecnica delle Marche), Ancona, Italy, in 2001, the University degree in astronautic engineering and Ph.D. in aerospace engineering from the “Sapienza” University of Rome, Italy, in 2007 and 2011, respectively. He received the University Master degree in composites materials and nanotechnologies in aerospace applications from the “Sapienza” University of Rome, Italy, in 2012. He is currently with the Telecom Italia Laboratory (TILAB), as a Researcher with Mobile Telecommunications and Neural Networks and collaborates with “Sapienza” University of Rome, where his research activities are related to EM fields and composite materials interaction. His current research is focused on electric conductive polymers and radar-absorbing structures modeling, manufacturing and testing.



Roberto Pastore was born in Naples, Italy, in 1977. He received the University degree in Physics from the University of Studies “Federico II” of Naples, Italy, in 2003, and the University Master degree in “Composites Materials and Nanotechnologies for Aerospace Applications” from the “Sapienza” University of Rome, Italy, in 2006. He’s currently on the Ph.D.Master degree in Aerospace Engineering with “Sapienza” University of Rome, where his research activities are related to carbon nanoparticles physics and nanocomposite materials characterization.



Mario Marchetti was born in San Marcello, Italy, on May 30, 1943. He received the University degree in aeronautical engineering from Milan Polytechnic, Milan, Italy, in 1972. He then joined the School of Aerospace Engineering, “Sapienza” University of Rome, Rome, Italy, where he is currently a Full Professor of the Engineering Faculty, in charge of the “Space Structures” course, the Director of the Department of Astronautic, Electric and Energetic Engineering, and is responsible for the SASLab laboratories.